Structural and vibrational analysis of indolyl radical and indolyl radical cation from density functional methods

Susan E. Walden and Ralph A. Wheeler *

Department of Chemistry and Biochemistry and the Center for Photonic and Electronic Materials and Devices, University of Oklahoma, 620 Parrington Oval, Room 208, Norman, OK 73019, USA

Electronic and structural properties of indole are the foundation for analyses of proteins based on the photochemistry and photophysics of the aromatic amino acid tryptophan. As the physiological importance of tryptophyl radicals and radicals of tryptophyl derivatives becomes apparent, the need for detailed information concerning indolyl radical and indolyl radical cation grows. Because of the high reactivity and very short life-span of these species, they are ideal targets for computational examination and prediction of properties to guide experimentalists. We have applied relatively new density functional based methods (SVWN, BLYP and B3LYP) to test their applicability and accuracy for this type of molecule. Although available experimental evidence for comparisons is scarce, our calculations exhibit excellent agreement with photochemically induced dynamic nuclear polarization (p-CIDNP), time-resolved resonance Raman (TR^3), and difference Fourier transform infrared spectroscopic (FTIR) experiments. We compare the geometries and vibrational modes of the radicals to the closed shell indole, to each other, and to available tryptophyl radical experimental information. We present the first complete set of assigned vibrational modes for indolyl radical and indolyl radical cation to further the applicability of vibrational spectroscopy for characterizing tryptophan radicals in proteins.

Introduction

The ubiquitous indole molecule is found in such varied places as coal tar distillates, perfumes,[1] and the evolutionarily conserved hormone melatonin.[2] In fact as the aromatic side chain of the amino acid tryptophan, its radical or radical cation is important in protein structure and function (*e.g.* cytochrome c peroxidase,[3-6] DNA photolyase[7-9] and galactose oxidase[10]) and in the etiology of chemical and radiative damage to proteins and DNA.[11-16] Melatonin is hypothesized to be an endogenous radical scavenger to help prevent oxidative damage of proteins and DNA associated with carcinogenicity and ageing.[2,17] The neurotransmitters serotonin and tryptamine both contain the electron-rich indole moiety as do many alkaloids which are pharmacologically important.[18-20] The facile one-electron oxidation of indole, reactions of the oxidized species (*i.e.* with $^3O_2$), and indole's potential function as an electron donor are properties which contribute to the differing biological functions of indole related molecules.[20-23] Materials science, particularly the field of organic polymeric conductors, is another vital area where knowledge of the oxidation chemistry and electronic properties of indole, indolyl radical, and indolyl radical cation has great potential.[24-27]

The precise biological roles for indole (IndH) or tryptophan (Trp) derived radicals have yet to be proven, in part due to the scarcity of information regarding the physical properties of the indolyl radical and indolyl radical cation. The electronic absorption spectra have been determined[28-34] for indolyl radical (Ind$^\bullet$, see **1a** for structure and atom numbering) and radical cation (IndH$^{\bullet+}$, **1b**) and tryptophyl radical (Trp$^\bullet$, **1c**) and radical cation (TrpH$^{\bullet+}$, **1d**), as have reduction potentials and pK_a values.[33-38] Photochemically induced dynamic nuclear polarization spectra (p-CIDNP), a specialized NMR technique, have shown the relative magnitudes and signs of isotropic hyperfine coupling constants for the protons for TrpH$^{\bullet+}$ and IndH$^{\bullet+}$.[39-43] An application of electron–nuclear double resonance (ENDOR) experiments on cytochrome c peroxidase compound ES resulted in proposed spin densities for some of the heavy atoms of a TrpH$^{\bullet+}$.[5] Because of their high reactivity, a structure

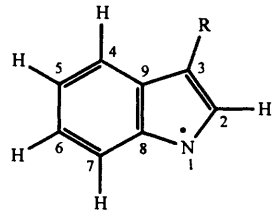

1a Ind$^\bullet$ R=H
1c Trp$^\bullet$ R=alanyl

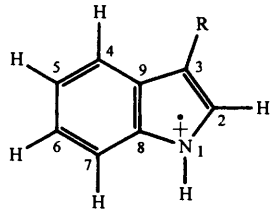

1b IndH$^{\bullet+}$ R=H
1d TrpH$^{\bullet+}$ R=alanyl

is not known for either radical, nor are there precise, total distributions of spin densities. Only limited and tentative assignments exist for the vibrational spectrum of Trp$^\bullet$ (3 fundamentals) and TrpH$^{\bullet+}$ (1 fundamental).[44,45]

The p-CIDNP experiments show the proton isotropic hyperfine coupling constants, and through the McConnell relation the spin densities on the heavy atoms, for the radical cations of both indole and tryptophan to be in the order $3 \gg 2 \sim 4 \sim 6 > 1 \gg 7 > 5$, with 3, 2, 4, 6 and 1 being positive, 5 being negative, but practically zero, and 7 essentially zero.[39-43] C7 shows a very small positive enhancement in some derivatives of Trp[42,43] and as there is no H3 in TrpH$^{\bullet+}$ that enhancement is only observed for IndH$^{\bullet+}$. The large emissive enhancement for β-CH_2, however, correlates with a very large spin density at C3.[39,40,42] The recent ENDOR experiments on cytochrome c peroxidase compound ES[5] differ from the p-CIDNP by reporting no observed spin density on C4 or C6 where significant enhancements are observed in the p-CIDNP experiments. In addition, the ENDOR derived spin density for C3 is not significantly greater than the C2 spin density and, though no spin density is reported for C7, a very small spin density is reported for C5 and assigned a negative sign based on Hückel–McLachlan calculations. We recently reported preliminary calculations on radicals derived from indole, including geometries, spin densities and a single vibrational mode from density functional methods.[46] Additionally, calculations on radicals derived

from 3-methylindole have been reported including a small selection of the 51 IR and Raman active vibrational frequencies.[47]

Although Asher and co-workers reported the observation of 'tryptophan transients' in a saturated UV resonance Raman experiment on Trp,[48] to our knowledge no complete assignment of the vibrational modes for Ind$^{\bullet}$, IndH$^{\bullet+}$, Trp$^{\bullet}$, nor TrpH$^{\bullet+}$ exists in the literature. In time-resolved resonance Raman (TR^3) experiments,[44] Bisby and co-workers showed that with long wavelength excitation (580 nm, TrpH$^{\bullet+}$; 520 nm, Trp$^{\bullet}$) the TR^3 spectra of the two species are distinguishably different. In addition, Berthomieu and Boussac[45] examined amino acid radicals including Trp$^{\bullet}$ by difference FTIR and tentatively assigned three modes of Trp$^{\bullet}$. Although the full vibrational spectra for the different radical species have not been assigned, interest in these spectra is growing rapidly because of the utility of Trp UV resonance Raman spectra for characterization of proteins.[49] We have thus undertaken a complete analysis and characterization of the vibrational modes of Ind$^{\bullet}$ and IndH$^{\bullet+}$ including comparisons between the two radical species and with the assigned modes of indole[50] and Trp.

To aid the identification and investigation of Ind$^{\bullet}$, IndH$^{\bullet+}$, Trp$^{\bullet}$, and TrpH$^{\bullet+}$, we recently presented and published structures, spin densities, and a single, distinguishing vibrational frequency for Ind$^{\bullet}$ and IndH$^{\bullet+}$ calculated with the local density approximation method of Slater,[51] Vosko, Wilk and Nusair[52] (SVWN) and the gradient-corrected method comprising Becke's exchange functional[53] and the correlation functional of Lee, Yang and Parr[54] (BLYP). (A more detailed explanation of the methods and procedures used for the calculations is given in the Appendix.) Because several groups have suggested that the hybrid Hartree–Fock/density functional theory method B3LYP[55] yields better geometries and spin properties,[56–59] we now include the geometry and spin densities calculated with that method and compare with our previous report. For all three methods, in addition to the complete calculated and assigned vibrational spectra for Ind$^{\bullet}$ and IndH$^{\bullet+}$, we also now present the rotational constants, dipole moments and predicted isotropic hyperfine coupling constants based on the Fermi contact spin densities.

Results and discussion

Geometries, rotational constants and dipole moments

In our earlier reports,[46,50] the geometry of indole was compared to experimental data and, based on the predicted rotational constants, B3LYP seemed to provide the most accurate geometry. As there are no experimental data for Ind$^{\bullet}$ and IndH$^{\bullet+}$ with which to compare the calculated structures, rotational constants and dipole moments, we present predicted structures from our calculations to assist the future analysis of experimental data. We will discuss the changes resulting from the oxidation of indole (IndH) to form the radical cation (IndH ⟶ IndH$^{\bullet+}$) and the removal of a hydrogen atom to form the neutral radical (IndH ⟶ Ind$^{\bullet}$).

The calculated bond lengths are given in Table 1 for IndH, Ind$^{\bullet}$ and IndH$^{\bullet+}$ for each method used here, SVWN, BLYP and B3LYP with the 6-13G(d) basis set[60] and for a B3LYP calculation which was carried out with a larger 6-311G(d,p) basis set. For indole, calculated bond distances have been described in detail elsewhere.[50] Likewise qualitative trends for the bond length differences of the radicals have been discussed previously for calculations with the SVWN method. We now include B3LYP bond distances since these are more accurate for IndH and have not previously been reported for the radicals. With only one exception (C8–C9, discussed below) the trends observed in bond length changes from IndH to each of the radical species hold across all methods and the two basis sets. So even if the predicted structures are improved upon later, we are confident that the calculated changes in bonding resulting from the electronic changes are qualitatively correct.

For IndH$^{\bullet+}$, bond distance changes relative to indole, except C8–C9, have been explained based on the nodal structure of indole's HOMO obtained from a UHF calculation with a 6-31G(d) basis set, and shown in **2**.[46] In general, bonding interactions in **2** result in a lengthened bond in IndH$^{\bullet+}$, while antibonding interactions in **2** result in a shortened bond in IndH$^{\bullet+}$. The most significant bond length changes occur within the pyrrolic ring as one NC bond contracts by 0.046 Å (N1–C2) and the other expands by 0.028 Å (C8–N1). Similarly, C2–C3 lengthens by 0.054 Å while C3–C9 shortens by 0.032 Å. The C6–C7 bond in the six-membered ring also exhibits a considerable expansion of 0.033 Å. These bond length changes will help explain shifts in the vibrational spectra. For the C8–C9 ring

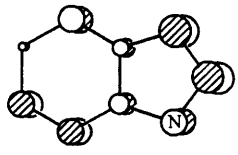

HOMO for IndH

2

Table 1 Bond lengths (in Å) for indole, indolyl radical and indolyl radical cation calculated by DF and HF/DF methods with the 6-31G(d) basis set except where noted

	SVWN			BLYP			B3LYP			B3LYP/6-311G(d,p)		
Bond	IndH	Ind$^{\bullet}$	IndH$^{\bullet+}$	IndH	Ind$^{\bullet}$	IndH$^{\bullet+}$	IndH	Ind$^{\bullet}$	IndH$^{\bullet+}$	IndH	Ind$^{\bullet}$	IndH$^{\bullet+}$
N1–C2	1.371	1.321	1.335	1.396	1.338	1.352	1.383	1.319	1.337	1.382	1.317	1.333
C2–C3	1.369	1.426	1.414	1.381	1.444	1.430	1.370	1.438	1.424	1.367	1.436	1.422
C3–C9	1.424	1.415	1.403	1.444	1.434	1.420	1.438	1.427	1.407	1.436	1.425	1.405
C9–C4	1.399	1.393	1.409	1.413	1.409	1.427	1.406	1.398	1.419	1.404	1.396	1.417
C4–C5	1.384	1.398	1.393	1.400	1.416	1.410	1.388	1.404	1.396	1.387	1.402	1.394
C5–C6	1.403	1.390	1.391	1.419	1.405	1.406	1.410	1.396	1.398	1.408	1.393	1.396
C6–C7	1.385	1.408	1.416	1.401	1.426	1.434	1.390	1.414	1.423	1.387	1.411	1.421
C7–C8	1.391	1.376	1.373	1.407	1.390	1.387	1.399	1.380	1.374	1.397	1.377	1.371
C8–C9	1.421	1.428	1.417	1.438	1.442	1.435	1.424	1.429	1.426	1.422	1.426	1.424
C8–N1	1.369	1.394	1.391	1.392	1.425	1.418	1.380	1.415	1.408	1.379	1.413	1.407
N1–N10	1.017	N/a	1.024	1.016	N/a	1.022	1.008	N/a	1.014	1.005	N/a	1.013
C2–H11	1.090	1.095	1.092	1.089	1.091	1.089	1.081	1.086	1.082	1.079	1.083	1.080
C3–H12	1.090	1.094	1.092	1.089	1.091	1.089	1.081	1.083	1.083	1.079	1.082	1.080
C4–H13	1.096	1.097	1.096	1.095	1.095	1.092	1.087	1.087	1.085	1.084	1.085	1.083
C5–H14	1.096	1.095	1.094	1.094	1.093	1.092	1.087	1.087	1.085	1.085	1.084	1.082
C6–H15	1.096	1.096	1.095	1.094	1.094	1.093	1.087	1.087	1.085	1.084	1.084	1.083
C7–H16	1.096	1.096	1.096	1.095	1.093	1.092	1.087	1.086	1.085	1.085	1.084	1.083

fusion bond, SVWN and BLYP show a contraction and B3LYP (with both basis sets) shows an expansion for this bond for $IndH^{\bullet+}$. Because of the bonding character of indole's HOMO for C8–C9, see **2**, the differing result from B3LYP appears to reflect the mixing of Hartree–Fock with DF exchange. However, the magnitude of the changes are 0.004 Å or less and the average absolute value is less than 0.003 Å. Thus, within the limits of the theory (accuracy approximately within 0.005 Å)[50,61,62] these bond lengths are essentially the same and there is no real disagreement between methods.

For $Ind^{\bullet}$, no simple pattern of bond length changes is evident. As for $IndH^{\bullet+}$, the changes are more pronounced within the five-membered ring of $Ind^{\bullet}$, N1–C2 contracts by 0.064 Å (to 1.319 Å) and C8–N1 expands by 0.035 Å (to 1.415 Å). The C2–C3 bond distance exhibits the largest change, as it expands by 0.068 to 1.438 Å. The change in C3–C9 is smaller with a contraction by 0.011 to 1.427 Å. The most impressive change in bond distance within the benzene ring is again for the C6–C7 bond, though the change is smaller than for $IndH^{\bullet+}$.

Comparing calculated bond distance changes for $IndH^{\bullet+}$ and $Ind^{\bullet}$ relative to indole reveals several important features. First, the largest changes in bond distances (usually greater than 0.01 and as large as 0.068 Å) occur within the five-membered pyrrolic ring for both $IndH^{\bullet+}$ and $Ind^{\bullet}$. Second, except for C9–C4 and C3–C9 the expansion or contraction of a particular bond is the same for $IndH^{\bullet+}$ and $Ind^{\bullet}$, in both direction and approximate relative magnitude. For the exceptions, C9–C4 expands by more than 0.01 Å for $IndH^{\bullet+}$, but contracts slightly for $Ind^{\bullet}$ and C3–C9 contracts three times as much in $IndH^{\bullet+}$ as in $Ind^{\bullet}$.

Table 2 shows the calculated rotational constants and dipole moments for $Ind^{\bullet}$ and $IndH^{\bullet+}$, again for each method and basis set tested. All methods and basis sets show that the three rotational constants, *A*, *B* and *C* (in MHz) for $IndH^{\bullet+}$ are smaller than those for $Ind^{\bullet}$. Though the predicted rotational contants for a particular radical vary depending on the method/basis set used, the differences for each constant between $Ind^{\bullet}$ and $IndH^{\bullet+}$ are very similar among the different methods. The difference in *A* between $Ind^{\bullet}$ and $IndH^{\bullet+}$ ranges from 79.54 to 93.6 MHz in value, but the $IndH^{\bullet+}/Ind^{\bullet} \times 100$ percentage ratios only range between 97.6% for B3LYP [6-311G(d,p)] to 98.0% for BLYP. The rotational constants *B* and *C* are similarly smaller for $IndH^{\bullet+}$ than $Ind^{\bullet}$ with percentage ratios ranging from 97.9 to 98.1%.

For the calculated total dipole moment (in Debye) from all methods and basis sets considered here, $\mu(IndH^{\bullet+})$ is greater than $\mu(Ind^{\bullet})$. Particularly striking is the difference in the *x* component for the two radical species where the value for $IndH^{\bullet+}$ is large and negative and the value for $Ind^{\bullet}$ is small and positive.

The differences in rotational constants and dipole moments, especially the *x* components, could aid in identifying or distinguishing the two radical species of IndH.

Spin properties of $IndH^{\bullet+}$ and $Ind^{\bullet}$

The trend in atomic spin densities for $IndH^{\bullet+}$ excluding C8 and C9 (Table 3), calculated by using the SVWN and BLYP methods, is C3 > C4 > C6 > C2 ~ N1 ~ C7 > C5, whereas B3LYP calculations show a very slightly different trend of C3 > C4 > C6 > C2 > N1 > C7 > C5 differing only in relative magnitude for C2, N1 and C7. While the reported trend for $IndH^{\bullet+}$ and $TrpH^{\bullet+}$ from p-CIDNP experiments shown earlier states that C2 ~ C4 ~ C6 and C7 is essentially zero, a schematic representation[40] and the published difference spectra themselves[40,42,43] reveal that the C2 enhancement and thus, spin density, is slightly less than that for C4 and C6 and that there is a discernible, though small, set of peaks from the C7 proton. Our calculated spin densities for $IndH^{\bullet+}$ correlate very well with the published difference spectra and, thus, show favourable agreement with the p-CIDNP experiments. We note, however, that our calculated spin densities for $IndH^{\bullet+}$ differ from those experimentally determined for $TrpH^{\bullet+}$ (in Ccp compound ES),[5] which are C2 = 0.35, C3 = 0.41, C5 = (−)0.07 and N1 = 0.14. These investigators did not observe what we have calculated to be significant spin density on C4

Table 2 Rotational constants (in MHz) and dipole moments (in Debye) for indolyl radical and indolyl radical cation calculated with DF and HF/DF methods using the 6-31G(d) basis set (except where otherwise noted)

Rotational constants	SVWN		BLYP		B3LYP		B3LYP/6-311G(d,p)	
	$Ind^{\bullet}$	$IndH^{\bullet+}$	$Ind^{\bullet}$	$IndH^{\bullet+}$	$Ind^{\bullet}$	$IndH^{\bullet+}$	$Ind^{\bullet}$	$IndH^{\bullet+}$
A	3985.3605	3901.3765	3897.4614	3817.9213	3958.8940	3867.5347	3974.8570	3881.2165
B	1679.8573	1643.9569	1636.8391	1602.7287	1660.8919	1629.2809	1665.3803	1643.4328
C	1181.7439	1156.5939	1152.7233	1128.8484	1170.0259	1146.3547	1173.6472	1150.1071
Dipole moments								
x	0.3525	−2.1279	0.2902	−1.5571	0.1465	−1.7397	0.1050	−1.7758
y	−2.4364	−1.2632	−2.3466	1.8900	−2.3764	1.9517	−2.3748	1.9623
z	0.0000	0.0058	0.0000	0.0000	0.0000	0.0000	0.0000	0.0000
μ(total)	2.4618	2.4746	2.3645	2.4488	2.3809	2.6145	2.3771	2.6465

Table 3 Spin densities for indolyl radical and indolyl radical cation calculated with DF and HF/DF methods using the 6-31G(d) basis set (except where noted)

	SVWN		BLYP		B3LYP		B3LYP/6-311G(d,p)	
	$Ind^{\bullet}$	$IndH^{\bullet+}$	$Ind^{\bullet}$	$IndH^{\bullet+}$	$Ind^{\bullet}$	$IndH^{\bullet+}$	$Ind^{\bullet}$	$IndH^{\bullet+}$
N1	0.23	0.12	0.26	0.12	0.28	0.11	0.28	0.11
C2	−0.03	0.14	−0.07	0.14	−0.12	0.17	−0.11	0.17
C3	0.48	0.30	0.54	0.32	0.61	0.34	0.61	0.35
C4	0.19	0.24	0.21	0.27	0.23	0.30	0.22	0.29
C5	−0.02	−0.04	−0.04	−0.07	−0.07	−0.11	−0.06	−0.11
C6	0.15	0.17	0.16	0.19	0.18	0.23	0.18	0.23
C7	0.06	0.13	0.05	0.12	0.01	0.08	0.02	0.08
C8	0.04	0.01	0.04	0.01	0.06	0.03	0.06	0.03
C9	−0.06	−0.04	−0.10	−0.06	−0.15	−0.09	−0.14	−0.09

and C6, nor did they observe the small spin density predicted for C7. Our values for C5 and N1 are quite similar to their measured ones, but they report C2 and C3 as having similar spin densities, where our calculations show the C3 spin density to be roughly twice the C2 spin density. While this could indicate a misrepresentation of the spin density distribution by the methods or the basis set chosen or indicate that the CH_2 substituent at C3 of $TrpH^{\bullet+}$ severely alters the spin distribution, the differences could also arise due to the environment of the protein. One might also argue that the disagreement between calculated spin densities for $IndH^{\bullet+}$ and experimental spin densities for $TrpH^{\bullet+}$ lies with the Mulliken population analysis[63,64] used to calculate these spin densities; however, use of Bader's AIM algorithm[65] did not show appreciable changes in magnitudes and did not change the observed trends. Likewise, the B3LYP calculations with the larger basis set, showed changes no larger than 0.01 from the B3LYP spin densities calculated with the 6-31G(d) basis.

For $Ind^{\bullet}$ the trend in calculated spin densities follows the pattern C3 ≫ N1 > C4 > C6 > C7 > C5 > C2, where C7 is very small and positive and C5 and C2 are very small and negative. For B3LYP, though, the predicted spin for C2 has become significant at −0.12. To our knowledge there are no experimental spin densities for $Ind^{\bullet}$ with which to compare our calculated values. Our results are consistent, however, with the observations that radical attack and coupling occurs only at C3 for $Ind^{\bullet}$.[66]

While the trends for spin densities differ little among the methods for each radical, the magnitudes show small numerical variations which can be up to a 250% relative change between SVWN and B3LYP with BLYP magnitudes generally in between the other two. Thus, except for C7, positive spin densities predicted by SVWN are more positive from B3LYP and negative spin densities from SVWN are more negative by B3LYP.

To our knowledge neither experimental nor calculated isotropic hyperfine coupling constants are available in the literature for $Ind^{\bullet}$ and $IndH^{\bullet+}$. The recently reported total hyperfine coupling constants for ring protons of $TrpH^{\bullet+}$ are not the isotropic coupling constants and thus, are not truly comparable to our calculations.[5] Several recent reports have concluded that the inclusion of Hartree-Fock exchange in the hybrid HF/DF method improves the hyperfine properties predicted for radicals by density functional theory.[56,57,67] Although most calculations of isotropic hfcc by density functional methods have utilized very large basis sets, Cohen and Chong found that B3LYP with the 6-31G* basis is capable of giving values differing from experiment by less than 15%.

We have included in Table 4 our SVWN, BLYP and B3LYP calculated isotropic hyperfine coupling constants (hfcc). The different functionals and the two basis sets predict quite different hfcc for some atoms. In places there is even disagreement in the sign of an hfcc for a particular atom. It is unfortunate that experimental data are not available to assess the quality of the different methods. Our past experience indicates that the quantitative agreement is likely within 20% for the B3LYP results.[59,69] Nevertheless, for all the methods, the relative difference between $Ind^{\bullet}$ and $IndH^{\bullet+}$ hfcc is the same for any given atom. We expect that these calculated hfcc are at least qualitatively correct and provide a first approximation for simulation of experimental spectra.

Vibrational frequencies and assignments

Although recent literature suggests that the B3LYP method may be preferable for calculations of vibrational frequencies,[55,58,59,69] analysis of some results in our laboratory, including indole,[50] and in others[70] shows that the BLYP method yields vibrational frequencies in better accord with experiment. If the uniform frequency scaling factor of Pulay[70] (0.963) is applied to the B3LYP frequencies of IndH, they show very close agreement with experiment and with BLYP calculated frequencies. While scaling could be applied to B3LYP frequencies for $Ind^{\bullet}$ and $IndH^{\bullet+}$, the scaling factor was not determined or tested for open shell molecules. Scaling the B3LYP frequencies of the radicals in this manner, however, does bring them extremely close to the BLYP frequencies. Because of the closer agreement of BLYP frequencies with experiment for indole[50] and their similarity to the scaled B3LYP frequencies for the radicals themselves, the analysis here will focus on unscaled BLYP calculated frequencies. The frequencies from the various computational methods and the minor variations in the assignments are all shown in the tables (Tables 5 and 6) to illustrate the consistency of the attribution of various frequencies to specific vibrations.

For the discussion of the vibrational modes certain conventions have been followed: (*i*) the benzene ring of indole is sometimes referred to as Φ, while the pyrrole ring and its vibrations are sometimes designated with Π; (*ii*) the abbreviations ν, δ and γ represent stretching, in-plane bending, and out-of-plane bending or wagging, respectively; (*iii*) reference is frequently made to the Wilson modes of benzene in the manner, ν9b for example, indicating similarity to the 9b mode of an *ortho*-disubstituted benzene ring;[71,72] and (*iv*) reference is made to vibrational modes of tryptophan using the W# convention of physical biochemists.[49]

Table 4 Isotropic hyperfine coupling constants (in Gauss) for the heavy atoms (^{14}N, ^{15}N and ^{13}C) and hydrogens of indolyl radical and indolyl radical cation calculated with DF and HF/DF methods using the 6-31G(d) basis set (except where noted)

	SVWN		BLYP		B3LYP		B3LYP/6-311G(d,p)	
	$Ind^{\bullet}$	$IndH^{\bullet+}$	$Ind^{\bullet}$	$IndH^{\bullet+}$	$Ind^{\bullet}$	$IndH^{\bullet+}$	$Ind^{\bullet}$	$IndH^{\bullet+}$
$^{14}N1$	2.1	0.95	3.6	1.8	4.6	1.9	2.7	0.98
$^{15}N1$	3.0	1.3	5.1	2.5	6.5	2.7	3.9	1.4
C2	−4.7	0.12	−6.1	2.6	8.9	3.7	−9.6	−0.79
C3	11.2	6.0	20.9	11.5	26.1	13.0	13.6	5.6
C4	4.0	5.2	7.8	10.2	9.6	12.3	5.2	6.5
C5	−2.4	−3.1	−3.2	−4.4	−4.8	−6.9	−4.6	−6.3
C6	2.6	3.0	5.4	6.4	7.0	9.0	3.4	4.5
C7	−0.12	1.5	0.44	3.4	−1.1	1.7	−2.1	−1.0
C8	−0.90	−1.4	0.54	0.66	1.6	0.48	−0.36	−0.60
C9	−5.4	−4.1	−7.0	−5.0	−9.7	−6.5	−9.8	−7.3
H1	N/a	−3.0	N/a	−3.7	N/a	−3.8	N/a	−3.6
H2	−0.86	−3.4	0.0	−4.2	0.83	−5.1	0.72	−4.6
H3	−8.9	−6.1	−11.9	−7.7	−14.1	−8.5	−12.7	−7.8
H4	−3.6	−4.7	−4.7	−6.2	−5.3	−7.1	−4.6	−6.3
H5	−0.25	−0.03	0.31	0.80	1.02	1.9	0.82	1.6
H6	−2.9	−3.5	−3.8	−4.6	−4.4	−5.8	−3.9	−5.2
H7	−1.4	−2.5	−1.2	−2.9	−0.50	−2.0	−0.53	−1.8

Table 5 Calculated frequencies (cm^{-1}), IR intensities and mode descriptions for indolyl radical from DF and HF/DF methods with 6-31G(d) basis set[a]

SVWN	int.	BLYP	int.	B3LYP	int.	Approximate description
3179	6.4	3161	20.1	3249	15.5	**C3H** & C2H sym. stretch
3154	6.1	3134	15.6	3221	12.0	Φ 2 **C7H** > C6H > C5H > C4H
3151	8.1	3132	19.2	3219	15.1	**C2H** & C3H asym. stretch
3147	7.4	3125	30.3	3211	25.8	Φ asym. CH str. **C5H > C7H** > C4H > C6H
3134	4.8	3111	15.4	3198	13.4	Φ asym. CH str. **C6H, C4H** > C7H ≫ C5H
3126	2.0	3102	1.1	3189	0.3	Φ *ν* 13 **C4H, C5H** > C6H ≫ C7H
1641	3.0	1583	2.3	1646	3.8	~Φ 8a & C7–C8 *ν*
1623	28.8	1560	26.9	1621	36.3	~Φ 8b & sm. 8a
1478	9.2	1457	7.8	1508	8.8	~Φ **19a** & Π C3–C9 *ν*
1505	3.6	1434	0.1	1485	0.7	~Φ 19b, N1–C2 & C3–C9 *ν*, C2H *δ*
1437*	5.2	1422	9.4	1475	7.1	**N1–C2** & C5–C6 *ν*; C2H, C3H, C4H, C5H *δ* *more Φ than Π
1403	5.5	1351	7.0	1387	7.2	~Φ 14; C3H & C2H *δ*
1334	11.0	1317	6.0	1357	7.6	**C2H** *δ*; C2–C3 *ν*; sm. N1–C8 *ν*; sm. Φ CH *δ*
1288*	9.1	1267	5.7	1311	5.1	~Φ **3** & N1–C2 *ν* *& C3–C9 *ν*
1242	9.3	1205	5.1	1242	6.0	**C3–C9** & N1–C2 *ν*, Φ CH *δ*: **C4H, C5H** > C6H, C7H
1202	23.0	1177	19.2	1214	30.0	**C2H, C3H** *δ* (rock) & sm. N1C2 *ν* & C4H *δ*
1140	2.2	1150	3.8	1180	3.3	Φ CH *δ* except C-4-H
1167†	1.4	1126	3.0	1171*	3.5	**N1–C8** *ν*, **C4H, C5H** *δ* (scissor); sm. C2H, C3H *δ*; *+C6H & C7H *δ* (scissor) †Φ smaller Π*δ* larger than BLYP
1078	0.02	1063	0.5	1101	0.3	~Φ **9b** & sm. C2H, C3H *δ* (scissor)
1024	1.1	1003	0.2	1035	0.2	~Φ **18b**
988	0.8	961	1.6	980	2.5	**C2–C3** *ν*, C2H, C3H *δ* (scissor)
935	0.9	931	0.7	974	0.7	a″ Φ 5 (CH*γ*)
910	5.4	906	3.9	944	4.4	a″ Φ 10a (CH*γ*)
879	1.1	869	1.5	907	2.3	a″ **C2H** *γ*, Φ 10b, v. sm. C3H *γ* (asynch.)
878	1.8	869	1.0	896	0.8	Π and Φ skeleton *δ*
844	0.05	844	0.4	879	0.2	a″ Φ **10b**, C2H *γ*, v. sm. C3H *γ* (asynch.)
852	8.6	831	7.5	855	7.6	N1–C8 *ν*, Π and Φ ring *δ*
761	52.1	751	52	751	52	a″ **C3H** *γ*, Π and Φ (11) CH *γ* (all in-phase)
766	2.4	747	1.9	770	2.4	Π and Φ in-phase breathing
747	7.1	738	0.5	761	0.03	a″ **C8–C9 torsion**, Φ ring *γ*, and sm. Π ring *γ*
720	14.2	718	4.2	740	2.0	a″ **C3H** *γ*, Φ (11) CH*γ*, >C2H *γ*
575	0.2	569	0.2	586	0.3	Π and Φ skeleton *δ*
541	1.1	544	0.2	572	0.4	a″ ~ Φ **16a** and Π ring *γ*
534	0.5	530	0.2	545	0.1	~*F* **6a** and ~ breathing mode for Π ring
528	0.3	526	0.1	542	0.2	a″ Π ring *γ* (butterfly) & Φ 16a
398	4.1	400	2.9	415	3.5	a″ Φ **16b**
394	4.4	393	4.0	406	4.7	in-plane skeleton rock
233	1.1	234	1.7	243	2.1	a″ butterfly w/ twist
194	5.7	197	4.2	204	4.8	a″ butterfly

[a] Frequencies in cm^{-1}, intensities are calculated IR itensities, in mode descriptions: Φ = phenyl ring, Π = pyrrole ring, Φ# = Wilson vibration nomenclature for benzene-like modes, *ν* = stretch, *δ* = angle in plane bend, *γ* = out of plane bend or torsion, sm. = small, sym. = symmetric, asym. = asymmetric, asynch. = asynchronous, **bold** type indicates predominant contribution.

To our knowledge, no assigned vibrational spectra, calculated or experimental, have been published for Ind$^{\bullet}$ or IndH$^{\bullet+}$, although such information could be quite enlightening given the growing prominence of Raman and UVRR spectroscopies for studying Trp, Trp$^{\bullet}$ and TrpH$^{\bullet+}$ in proteins.[49,73] Three groups have observed resonance Raman or IR spectra for Trp$^{\bullet}$ and/or TrpH$^{\bullet+}$, but no definitive mode assignments have been made.[44,45,48] Because of the absence of published experimental data for Ind$^{\bullet}$ and IndH$^{\bullet+}$ vibrations, comparisons will be made to published data for Trp$^{\bullet}$ and TrpH$^{\bullet+}$. Moreover, because of the growing importance of Trp$^{\bullet}$ and TrpH$^{\bullet+}$ in biochemistry, we focus our vibrational analysis on modes of Ind$^{\bullet}$ and IndH$^{\bullet+}$ potentially most useful for identifying or characterizing Trp$^{\bullet}$ and TrpH$^{\bullet+}$.

Figs. 1 and 2 show qualitative sketches of representative Ind$^{\bullet}$ and IndH$^{\bullet+}$ vibrational modes analogous to those modes used to characterize trp in proteins.[49] Additionally, Table 7 displays frequencies for these and other modes, determined experimentally for Trp and from our calculations for indole, Ind$^{\bullet}$ and IndH$^{\bullet+}$. Although the peptide chain of Trp and its radicals is likely to modify vibrational frequencies relative to those of the indole analogues, many modes shown in Fig. 1 are concentrated on the benzenoid ring of the radicals and are likely to be quite similar for Trp-based and Ind-based radicals. Although within journal space constraints we cannot discuss all vibrational modes for Ind$^{\bullet}$ and IndH$^{\bullet+}$, they have all been examined and assigned. The complete set of calculated vibrational frequencies with mode descriptions and IR intensities for each radical are included in Tables 5 and 6 since to our knowledge this information is currently unavailable from any other source.

Trp has two benzene CC stretching modes, denoted as 8a (or W1), appearing near 1622 cm^{-1}, and 8b (or W2), appearing at a lower frequency of 1579 cm^{-1}. Mode W2 also involves NH *δ* and is frequently used to indicate the extent of H-bonding to Trp in proteins.[49] Berthomieu and Boussac reported a vibrational band at 1612 cm^{-1} for Trp$^{\bullet}$ and assigned it to W2;[45] whereas, Bisby and co-workers observed a strong band at a lower frequency of 1589–1591 cm^{-1} and related it to W1.[44] Johnson, Ludwig and Asher reported an observed band for Trp$^{\bullet}$† at 1593 cm^{-1} and also one at 1646 cm^{-1} which was not reported by either of the other groups.[48] In their paper, Bisby and co-workers hypothesized that the 1646 cm^{-1} band could be from Trp singlet or triplet excitations resulting from the high laser power or from a vibration in resonance with the different excitation frequency utilized by Asher *et al.* in their resonance Raman experiments. Although considerable effort has been made to characterize the UV–VIS spectra of IndH$^{\bullet+}$ and TrpH$^{\bullet+}$,[28–34] the IR spectra have not been as thoroughly investigated. As mentioned in the introduction, Bisby and co-workers

† A reviewer pointed out that on the nanosecond timescale of this experiment the loss of a proton to form Trp$^{\bullet}$ after ionization is not likely to be observed. Thus, while Asher *et al.* referred to Trp radical and not radical cation, they quite possibly observed the radical cation. The reviewer also reiterates the possible presence of a triplet Trp species.

Table 6 Calculated frequencies (cm^{-1}), IR intensities, and mode descriptions for indolyl radical cation from DF and HF/DF methods with 6-31G(d) basis set[a]

SVWN	int.	BLYP	int.	B3LYP	int.	Approximate description
3509	173	3491	135	3601	166	NH ν
3217	27	3210	10.7	3290	11.7	**C2H** & C3H symmetric ν
3206	13.5	3198	6.8	3279	9.7	**C3H** & C2H asymmetric ν
3171	4.9	3160	0.02	3243	0.1	Φ 2 CH ν C5H ≫ C4H, C6H ≫ C7H
3160	5.2	3150	0.04	3234	0.4	Φ 20a CHν CH7H > C6H,C4H ≫ C5H
3153	0.1	3146	0.02	3229	0.02	Φ 7a CH ν C4H ≫ C7H > C5H > C6H
3150	1.4	3140	0.03	3223	0.2	Φ 13 CH ν C6H > C7H > C5H > C4H
1640	2.2	1581	2.2	1643	1.9	**~Φ 8a** & NH δ & C7–C8 ν
1615	15.0	1550	15.9	1614	25.5	**~Φ 8b** & small (sm.) C3H δ
1520**	23.8	1481	0.7	1535	7.7	**~Φ 19b** & NH δ & N1–C2 ν & sm. C3H δ; **N1–C2 ν large for SVWN
1485	35.5	1459	42.1	1509	45	**~Φ 19a** & C2–C3 ν
1472**	12.2	1443	32.5	1496	49.8	**C2H δ & N1–C2 ν**; & C3–C9 & sm. Φ 19a **no N1–C2 ν, and more Φ 19a
1437	21.9	1404	39	1450	40.6	**C8–C9 & N1–C8 ν; NH** and **C2H ν**, some Φ CH δ (mostly C4H δ)
1434	34.4	1358	19	*1383**	29.1	**~Φ 14** on ring but not much C5H δ & sm. C3H δ *C5H included
1364	26.9	1350	14	*1401*	14.6	**C3–C9** ν, C5H δ, C3H δ, sm. N1–C2 ν
1276	32.5	1258	11.3	1300	12.9	**C7H** and C4H δ; C9–C8 ν (~Φ 3), N1–C2 ν & C3–C9 ν
1225	54.3	1216	35.0	1250	36.7	**C3H** δ; C4H δ; NH δ
1162	1.0	1171	8.1	1199*	86.6	~Φ **15** *N1–C8 ν (present in BLYP but very slight; moderate in B3LYP)
1207	41.3	1158	69.3	1191*	49.8	**N1–C8** ν; **C6H** δ; NH δ; sm. C4H δ *lg. C5H & no C4H & very sm. NH δ
1146	19.9	1139	18.6	1179	11.8	**C2H** δ and NH δ
1092	0.9	1074	4.9	1112	3.5	~Φ 9b
1050	1.6	1040	0.9	1068	2.1	**C2–C3** ν; C2H & C3H δ (scissor)
1028	0.3	1005	3.8	1034	6.8	~Φ 18b
971	0.3	971	0.4	1011	0.6	a″ Φ 5 concentrated on H5 & H6
935	3.6	936	2.0	973	2.4	a″ Φ 10a concentrated on H4 & H7
891	1.1	882	0.4	923	0.7	a″ C2H & C3H γ (out of phase); Φ 10b
873	0.1	863	1.4	*886*	4.1	Π and Φ skeleton δ
861	1.7	858	1.9	*898**	1.2	a″ C2H & C3H γ (out of phase); Φ 10b; *no C3H γ
862	1.6	851	0.9	875	0.3	Π and Φ skeleton δ
788	34.0	785	36.4	822	39.7	a″ C2H & C3H γ (in phase)
743	23.2	748	19.2	774	22.0	a″ Φ **11**; C3H γ; sm. C8–C9 γ
766	0.3	746	0.8	769	1.8	indole breathing
718	23.6	714	8.2	736	11.5	**C8–C9** γ; Φ CH γ & sm. C3H γ
649	119	612	101.7	639	109.7	NH γ
586	1.4	579	1.2	599	1.4	Π and Φ skeleton δ (C8–C9 rock)
562	0.3	543	3.6	560	2.5	a″ Π ring γ & Φ 16a
522	1.6	517	2.1	530	2.1	~Φ 6a
500	8.9	502	12.4	519	12.7	a″ Φ **16a** & Π ring γ
387	1.7	387	1.5	399	2.0	in plane skeleton rock
382	8.5	386	6.5	399	7.3	a″ Φ 16b
234	1.9	235	1.8	242	2.0	a″ butterfly w/ a swist
196	7.9	195	6.9	200	7.8	a″ butterfly

[a] Frequencies in cm^{-1}, intensities are calculated IR intensities, in mode descriptons: Φ = phenyl ring, Π = pyrrole ring, Φ# = Wilson vibration nomenclature for benzene-like mobes, ν = stretch, δ = angle in plane bend, γ = out of plane bend or torsion, **bold** type indicates predominant contribution. Assignments and ordering are based on BLYP with significant deviations in assignment noted for other methods and reordered modes are indicated by a frequency in *italics*.

recorded a time-resolved resonance Raman spectrum for $TrpH^{\bullet+}$, but the only peak which they specifically describe is seen at 1609 cm^{-1} and attributed to a benzene CC stretching mode.[44]

For indole, the 8b mode is calculated to appear at a higher frequency (1613 cm^{-1}) than 8a (1572 cm^{-1}), in contrast to the empirical force-field calculations on which Trp assignments are based.[74] Indole 8b is calculated to mix slightly with pyrrole stretching, whereas 8a mixes with Π CH and NH bending. The opposite relative order, with 8a above 8b, is calculated for Ind$^{\bullet}$ and $IndH^{\bullet+}$, where 8a has increased slightly in frequency relative to IndH and the mode most similar to 8b has shifted to lower frequency by 53 cm^{-1} for Ind$^{\bullet}$ and by 63 cm^{-1} for $IndH^{\bullet+}$. These shifts can be rationalized on the basis of bond length changes. In the benzenoid rings of Ind$^{\bullet}$ and $IndH^{\bullet+}$, the lengths of the stretching bonds in 8a, C8–C9 and C5–C6, exhibit very small changes relative to IndH. The bond distances vary in opposite directions with the larger change being contraction of the C5–C6 bond. This results in a very slight increase in frequency for the 8a mode for both radicals.

There are two possible combinations of bond stretches which could be called Wilson mode 8b. The first is the combination of C4–C5 and C7–C8 stretching vibrations, while the second is the combination of C4–C9 and C6–C7 stretching vibrations. For $IndH^{\bullet+}$, which has a larger decrease in frequency for the 8b mode, three of these bonds expand and only the C7–C8 bond contracts. In fact from total energy distributions and visualization,‡ C7–C8 stretching is no longer a significant part of the lower frequency 8b vibration but is mixed with the higher frequency mode 8a. So 8b decreases in frequency for $IndH^{\bullet+}$ because bonds involved in the stretching motion expand and weaken relative to IndH. In contrast, Ind$^{\bullet}$ shows larger expansion for C4–C5 and less expansion for C6–C7 than $IndH^{\bullet+}$ plus, two of the bonds of interest here contract—C4–C9 by <0.01 Å and, again, C7–C8 by approximately 0.02 Å. Like $IndH^{\bullet+}$, the C7–C8 stretch is mixed with the higher frequency 8a mode. The resulting combination of two expanded bonds and one slightly contracted one results in the smaller downward shift of 8b for Ind$^{\bullet}$ than for $IndH^{\bullet+}$.

Calculated IR intensities, which cannot account for resonance effects or predict intensities in Raman experiments, for Ind$^{\bullet}$ and $IndH^{\bullet+}$ show that the lower frequency 8b band is

‡ The total energy distributions[75,76] resulted from converting the GAUSSIAN92/DFT[77] or GAUSSIAN94[78] force constant matrix output to a form which could be used as input for the program GAMESS[79,80] to calculate the total energy distribution based on a set of redundant internal coordinates. The program XMOL[81] was used for animated visualization of the GAUSSIAN output.

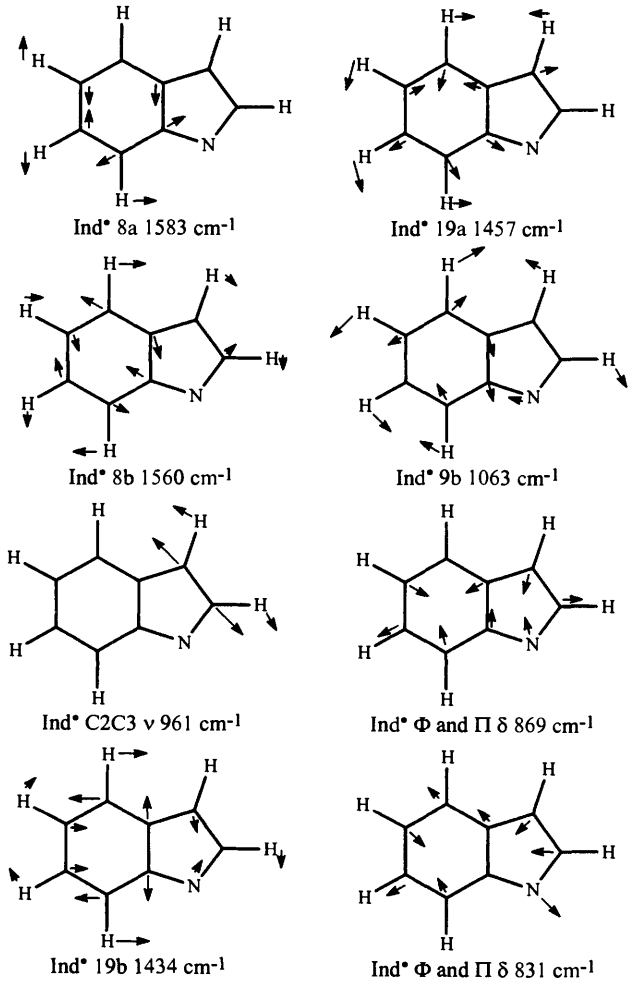

Fig. 1 Mode assignments calculated for Ind• with BLYP method and 6-31G(d) basis set. See text or Table 5 for key to symbols. Relative arrow lengths are approximately proportional to displacement.

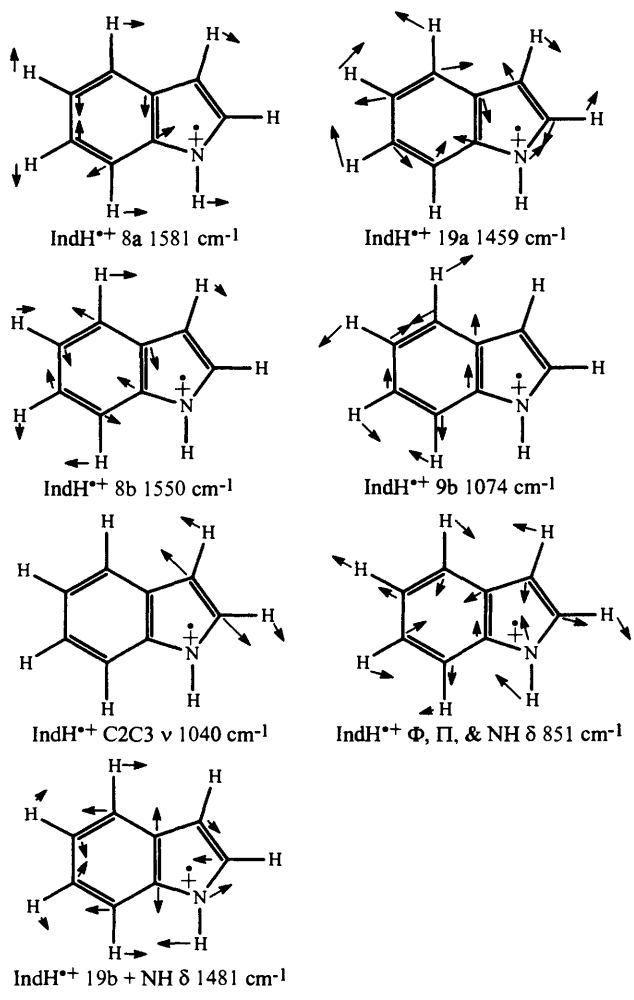

Fig. 2 Mode assignments calculated for IndH•+ with BLYP method and 6-31G(d) basis set. See text or Table 6 for key to symbols. Relative arrow lengths are approximately proportional to displacement.

much stronger, but the 8a band is also moderately intense so that both modes may be observable in difference FTIR spectroscopy. The calculated BLYP frequencies for Ind• support the assignment[44] of Bisby and co-workers of the observed *ca.* 1590 cm^{-1} band for Trp• as corresponding to benzene CC stretching which we assign as predominately Φ 8a (calculated frequency 1583 cm^{-1}).

What would seem to be the same vibration was reported at 1612 cm^{-1} by Berthomieu and Boussac from their low-temperature FTIR experiments,[45] though they related the band to W2 because of the observed shift when the solvent was changed from H_2O to D_2O. Although different techniques and solvents (50 : 50 v/v ethanol–water *versus* water) were used by the different groups, the experimental difference in frequency of *ca.* 20 cm^{-1} for this band of Trp• seems excessive and is not obviously explainable. Perhaps packing forces or hydrogen-bonding with the matrix (N as acceptor) increases the frequency of the mode in the low-temperature FTIR experiments.§

§ Another possible explanation is that the difference FTIR spectra are composed of superimposed Trp• and Trp•+ spectra. Upon examining the published spectra there are as many assigned and unassigned bands which are consistent with the IndH•+ calculations as there are bands consistent with Ind• calculations. The experiments were conducted in a buffer at pH (pD) = 12 which was frozen at 12 K prior to exposure to the ionizing radiation. While the pK_a of IndH•+ is *ca.* 4.6, the pK_a of IndH is near 16. The relative concentrations of Trp• to TrpH•+ after radiation would be determined by the relative proximity of a hydrogen-bonding hydrogen to either indolic nitrogen or aquatic oxygen. The reviewer's point concerning rate of proton transfer (see above) would seem to strengthen this explanation.

The band observed at 1612 cm^{-1} attributed to Trp• (ref. 45) is very close in frequency to the only assigned vibrational mode for TrpH•+ (benzene CC stretch) at 1609 cm^{-1} (ref. 44). Our calculations place this mode at 1581 cm^{-1} for IndH•+, a difference of 28 cm^{-1}, with a mode assignment of Wilson mode 8a mixed with NH bending. This difference could be within the error of the computational methods; however, for in-plane modes such as this, the root mean square deviation for the calculation of IndH frequencies by BLYP is 9 cm^{-1}. Another hypothesis involves hydrogen-bonding. Experimentally for Trp, W2, the lower frequency band of the 8a/8b pair is mixed with NH δ. We find the NH bend mixed with 8a for IndH and IndH•+. Thus the lower frequency band of the pair for IndH (as in Trp) and the higher frequency band of the pair for IndH•+ shows the NH bend and should be affected most by hydrogen-bonding. Since the NH δ mode is known to shift to higher frequency when the NH is involved in hydrogen-bonding,[49,82] hydrogen-bonding to the solvent in the time-resolved resonance Raman experiments could account for the difference between the experimental and calculated frequencies.

The C2–C3 stretching mode of Trp, labelled W3 and detected experimentally at 1552 cm^{-1}, is sensitive to the $X^{2,1}$ angle (C2–C3–C_β–C_α).[49] The corresponding mode of IndH was calculated[46,50] at 1514 cm^{-1} (exp. −1509 cm^{-1}),[83] composed of predominately C2–C3 stretch, but mixed with a small amount of Φ 19a. In contrast, Ind• calculations show two modes with C2–C3 stretching character, one at 1317 cm^{-1}, which is mostly C2–H δ, but with C2–C3 ν and C3–H δ and the other at 961 cm^{-1}, which

Table 7 Observed vibrational frequencies of Trp and corresponding calculated frequencies from BLYP/6-31G(d) for IndH, Ind$^{\bullet}$ and IndH$^{\bullet+}$.

Mode description[a]	Name	Trp (exp) cm^{-1}	IndH (calc.) cm^{-1}	Ind$^{\bullet}$ (calc.) cm^{-1}	IndH$^{\bullet+}$ (calc.) cm^{-1}
Φ ν_{8a} & ν NC8	W1	1622	1613 (8b)	1583 (8a)	1581 (8a & δ NH)
Φ ν_{8b}	W2	1579	1572 (8a & δ NH)	1560 (8b)	1550 (8b)
Π ν C2C3	W3	1552	1514	1317/961	1459/1040
Φ ν_{19b}	W4	1496	1450	1434	1481
Φ ν_{19a}	W5	1452	1492[b]	1457	1459
ν N1–C2 and C2–C3 (sym.) & δ NH	W6	1435	1414	1422	1443
Fermi doublet	W7	1362/1342	1357/1340[c]	?[d]/1351	?/1358
ν C3C9, δ NH	W8	1305	1269/1192	1205	1258 & 1350 (ν C3C9)
similar to $\Phi\nu_{9b}$	W13	1127	1119	1063	1074
Φ ring str. (resp)	W16	1012	1012 (Φ 18b)	1003 (Φ 18b)	1005 (Φ 18b)
sim $\Phi\nu_{12}$ & δNH	W17	879	882	869/831	851
Indole breathe	W18	759	753	747	746

[a] These mode descriptions and experimental frequencies are taken from J. C. Austin, T. Jordan and T. G. Spiro, in *Biomolec. Spectrosc., Part A*, ed. R. J. H. Clark and R. E. Hester, Wiley, New York, 1993, pp. 55–127 and references therein. Π = pyrrole ring localized; Φ = benzene ring localized. The Φ mode numbers are from Wilson. The calculated mode assignments were verified using the XVIBS and XMOL computer programs. [b] This caluclated frequency corresponds to Φ 19a, but it also is the one of the 1492/1450 cm^{-1} pair which has δ NH involvement and would be affected by H-bonding. [c] Calculated to be two fundamentals. [d] The motions exhibited in IndH have no precise matches in either radical.

is 50% C2–C3 ν, but with C3–H δ and C2–H δ. IndH$^{\bullet+}$ likewise shows substantial mixing of the C2–C3 stretch in two bands, one calculated at 1459 cm^{-1}, which is predominately Φ 19a but mixed with C2–C3 ν, and one at 1040 cm^{-1}, with similar mixing to the 961 cm^{-1} mode of Ind$^{\bullet}$.

Two other modes concentrated on the benzenoid ring, Wilson modes 19b and 19a, were measured for Trp at frequencies of 1496 and 1452 cm^{-1}, respectively.[49] Once again the ordering of these bands for Trp is based on an empirical force-field analysis.[74] A band of Trp$^{\bullet}$ reported by Berthomieu and Boussac at 1465 cm^{-1} is related to their Trp mode at 1456 cm^{-1}, which they described as indole C5–H δ. This Trp mode (W5) is alternatively described as benzene Wilson mode 19a.[49] The calculated order of these two modes, 19a and 19b, is reversed for both IndH (19a is calculated at 1492 and 19b at 1450 cm^{-1}) and Ind$^{\bullet}$ (19a appears at 1457 and 19b at 1434 cm^{-1}). For IndH$^{\bullet+}$, on the other hand, 19b is calculated to appear at a higher frequency (1481 cm^{-1}) than 19a (1459 cm^{-1}). The Φ 19b mode of Trp (W4, the higher of the pair) shows frequency shifts proportional with hydrogen-bonding, indicative of mode mixing with NH δ. Indeed, in our calculations, the higher frequency absorbance of the Φ 19 pair is mixed with NH δ for both IndH and IndH$^{\bullet+}$. However, for IndH this is the Φ 19a mode, yet for the radical cation it is the Φ 19b mode.

The pair of vibrational bands observed experimentally near 1350 cm^{-1} in Trp and IndH have been attributed to a Fermi doublet since Takeuchi and Harada presented their empirical force-field analysis of indole and skatole[74] and an experimental study of Trp derivatives, published with Miura.[84] This pair of vibrations in Trp is known to be sensitive to the indolic-ring environment, particularly the degree of hydrophobicity of the immediate surroundings.[49,84] In our previous report on indole,[50] we describe two calculated fundamentals in this region predicted by methods including electron correlation and note that molecular orbital methods not including correlation predict only one fundamental here. For IndH, the calculated frequencies are 1357 and 1340 cm^{-1}, which are assigned to a Φ and Π carbon (nitrogen)–hydrogen bending mode and Φ 14 with N1–C2 ν and a small amount of Π CH bends, respectively. The higher frequency mode is reminiscent of Φ 3 mixed with an analogous pyrrole mode asynchronously. Neither Ind$^{\bullet}$ nor IndH$^{\bullet+}$ is predicted to have a mode with similar displacements, though Ind$^{\bullet}$ does exhibit a Φ 3 mode mixed with N1–C2 ν at 1267 cm^{-1}. Ind$^{\bullet}$ is also predicted to have a mode at 1351 cm^{-1} nearly identical to the IndH mode at 1340 cm^{-1}, only the NH δ contribution is missing. For IndH$^{\bullet+}$, however, the Φ 14 mode is mixed only with very small amounts of C3–H δ and N1–C2 ν.

A band was observed at 1083 cm^{-1} for Trp$^{\bullet}$, believed to correspond to a Trp mode at 1071 cm^{-1}, which was tentatively assigned as the benzene 18b mode.[45] Our BLYP calculations instead predict the benzene 18b-like mode for Ind$^{\bullet}$ to be near 1003 cm^{-1}, a very small deviation from the predicted frequency for IndH of 1012 cm^{-1}. This mode for Ind$^{\bullet}$ shows a calculated, 10-fold decrease in IR intensity relative to indole. We suggest that the observed band at 1083 cm^{-1} for Trp$^{\bullet}$ may actually correspond to the Trp W13 mode (benzene 9b-like) observed at 1127 cm^{-1}. This mode is calculated by BLYP to appear at 1063 cm^{-1} for Ind$^{\bullet}$, display weak intensity, and, like 18b, involve benzene bending for both the ring and the CHs. Neither of these benzene modes is significantly different in frequency for IndH$^{\bullet+}$ relative to Ind$^{\bullet}$, with the 18b-like mode calculated to appear at 1005 cm^{-1} and the 9b-like mode calculated at 1074 cm^{-1}. There is, however, a calculated 10-fold increase in intensity for the bands of IndH$^{\bullet+}$ relative to those of Ind$^{\bullet}$. We note that the radicals, like indole, do not include significant pyrrole breathing-type motion in the calculated mode near 1010 cm^{-1}, although the corresponding mode for Trp has alternatively been described as the out-of-phase combination of Φ and Π breathing, despite the lack of shift with ^{15}N-substitution.[85]

The W17 mode of Trp, observed near 879 cm^{-1}, has proven useful for detecting hydrogen-bonding of the residue in proteins as it is resolvable *versus* other amino acid residues and is enhanced in UVRR spectra excited with the B_b electronic transition.[49] According to empirical force-field calculations,[74] this mode is attributed to benzene ring bending similar to Wilson mode 12 mixed with NH δ. We previously presented DF calculations for IndH indicating that this mode is actually Π ring bending mixed with NH δ (calc. at 882 cm^{-1}) and that the benzene mode 12 occurs at 861 cm^{-1}, without mixing with NH δ.[50] For Ind$^{\bullet}$, of course, there is no mixing with NH δ present, but Φ 12 and the Π ring δ mix, symmetrically and antisymmetrically, in two modes calculated at 869 and 831 cm^{-1}, respectively. As a potential indicator of H-bonding for IndH$^{\bullet+}$, these modes could be quite significant. In contrast to IndH, yet similar to Ind$^{\bullet}$, this type bending of the two rings is mixed into two modes calculated at 863 and 851 cm^{-1}. Only the lower frequency, 851 cm^{-1}, band is calculated to include NH δ, though it is unfortunately the less intense of the two modes.

In summary, although there is very little experimental data for the indolyl radicals of either indole or tryptophan, our calculations show good agreement with what is available. Additionally, because of the excellent agreement between the gradient-corrected DF calculated harmonic vibrational frequencies of IndH and IR and Raman experiments on indole and tryptophan, including experiments on isotopically substituted IndH and Trp, we believe the presented vibrational frequencies and assignments for Ind$^{\bullet}$ and IndH$^{\bullet+}$ to be qualitatively reasonable, and possibly quantitative, predictions for directing vibrational spectroscopic characterization of Ind$^{\bullet}$, IndH$^{\bullet+}$, Trp$^{\bullet}$ and TrpH$^{\bullet+}$.

Conclusions

The structures, spin properties, and vibrations of Ind$^{\bullet}$ and IndH$^{\bullet+}$ provide a basis for interpreting spectra of radicals derived from tryptophan and its derivatives. Although there are currently no experimental data for comparison, we report calculated structural data for the two species Ind$^{\bullet}$ and IndH$^{\bullet+}$, including bond lengths, rotational constants and dipole moments. The three computational methods all predict the same changes in bonding between either IndH$^{\bullet+}$ and IndH or Ind$^{\bullet}$ and IndH. The most notable changes in bond distance (>0.030 Å, B3LYP) are predicted for the N1–C2, C2–C3, C3–C9 and C6–C7 bonds of IndH$^{\bullet+}$ and for the N1–C2, C2–C3 and C8–N1 bonds of Ind$^{\bullet}$. The rotational constants and dipole moments may be distinguishably different for free indolyl radicals where the rotational constants calculated for IndH$^{\bullet+}$ are smaller than for Ind$^{\bullet}$ and the predicted total dipole moment of IndH$^{\bullet+}$ is larger than for Ind$^{\bullet}$. A significant difference is calculated for the x component of the dipole moment between the two radicals. These differences between the two radicals are very similar for each method used in these calculations.

Calculated spin densities for IndH$^{\bullet+}$ agree very well with p-CIDNP spectra of free TrpH$^{\bullet+}$ or IndH$^{\bullet+}$ but show more spin on the six-membered ring than ENDOR spectra of TrpH$^{\bullet+}$ imply for cytochrome c peroxidase compound ES. Perhaps the protein environment influences the spin distribution on the TrpH$^{\bullet+}$. Trends in calculated spin densities show very little dependence on method or basis set. Thus, the B3LYP spin densities reported here calculated with two different basis sets do not differ substantially from the SVWN and BLYP spin densities previously reported.

We present the first calculated or experimental vibrational frequencies and mode assignments for Ind$^{\bullet}$ and IndH$^{\bullet+}$. BLYP calculated frequencies for Ind$^{\bullet}$ more closely agree with experiment for Trp$^{\bullet}$ than those calculated by other methods. Our calculations support tentative experimental assignments for Trp$^{\bullet}$ vibrations at 1590 and 1465 cm^{-1} as W1 (benzene 8a) and W5 (benzene 19a) Trp modes, respectively. We suggest, however, that the experimentally observed mode at 1083 cm^{-1} for Trp$^{\bullet}$ is not a benzene 18b-type mode but instead is the benzene 9b-like mode, W13. Differences between the fundamental modes of IndH, Ind$^{\bullet}$ and IndH$^{\bullet+}$ are greatest in the modes predominantly involving pyrrole vibrations. In fact, the region roughly between 1000 and 1450 cm^{-1} which contains all a′ ring bending and stretching modes mixed with CH and NH bending modes exhibits a veritable scrambling of the vibrations associated with the fundamental modes. While only the C2–C3 mode, taken individually, is distinct enough from other modes and has a large enough shift to easily distinguish the two radicals without benefit of direct comparison, the spectra as a whole are quite different in the frequencies, relative IR intensities and the mode assignments.

Acknowledgements

We gratefully acknowledge the support of our work by the United States National Science Foundation (NSF) through Grant Number CHE-9419734 to R. A. W. and Grant Number OST-9550478 to the Center for Photonic and Electronic Materials and Devices. Additional vital support in the form of grants of supercomputer time was provided by the NSF's National Center for Supercomputing Applications and Cornell Theory Center. The Cornell Theory Center receives major funding from the NSF and New York State. Additional funding comes from the Advanced Research Projects Agency, the National Institutes of Health, IBM Corporation, and other members of the center's Corporate Research Institute. We are also grateful for supercomputer time made possible by support from IBM Corporation and the University of Oklahoma and from the NSF, Silicon Graphics, Inc., and the University of Oklahoma to the Supercomputing Laboratory for the Electronic Properties of Materials, part of the Center for Photonic and Electronic Materials and Devices. S. E. W. also acknowledges the Oklahoma State Regents for Higher Education, the Graduate College and the Department of Chemistry and Biochemistry of the University of Oklahoma for Centennial Fellowship support.

Appendix: Computational methods

The geometry optimizations and frequency calculations were accomplished with the computer programs GAUSSIAN92/DFT[77] and GAUSSIAN94[78] to solve the Hartree-Fock[86,87] and Kohn–Sham[88,89] equations. The density-functional methods utilized embody the local density approximation for exchange of Slater[51] with the local correlation functional of Vosko, Wilk and Nusair[52] (SVWN) and Becke's gradient-corrected exchange functional[53] with the gradient-corrected correlation functional of Lee, Yang and Parr (BLYP).[54] These two methods are collectively referred to as DF methods. In addition, the three parameter, hybrid Hartree–Fock/density-functional (HF/DF) method derived from the BLYP, known as B3LYP,[55] was also employed. Unrestricted Hartree–Fock *ab initio* calculations (UHF) were also performed for comparison. All calculations were performed with the spin-unrestricted formalism and the 6-31G(d) basis set.[60] A geometry optimization was also made with the 6-311G(d,p) basis set and the B3LYP method to compare with the smaller basis set.

The starting geometry employed for all optimizations resulted from a semi-empirical MNDO[90] optimization, calculated using the program MOPAC 6.0.[91] Initially, the geometry was optimized in UHF and SVWN without any symmetry constraints. Because these resulted in a C_s symmetry optimized structure, subsequent calculations designated C_s symmetry for the molecule. Berny's optimization algorithm[92] in internal coordinates was used to fully optimize the geometries for each method before frequency calculations were performed. Analytical first derivatives and analytical or numerical second derivatives of the energy were computed for calculating harmonic force constants. The mode assignments were made through visualization of the atomic displacements with the program XMOL.[81]

References

1 G. Vernin and G. Vernin, in *Chemistry of Heterocyclic Compounds in Flavours and Aromas*, ed. G. Vernin, Ellis Horwood Ltd., Chichester, 1982, p. 135.
2 B. Poeggeler, R. J. Reiter, D. X. Tan, L. D. Chen and L. C. Manchester, *J. Pineal Res.*, 1993, **14**, 151.
3 P. S. Ho, B. M. Hoffman, C. H. Kang and E. Margoliash, *J. Biol. Chem.*, 1983, **258**, 4356.
4 A. L. P. Houseman, P. E. Doan, D. B. Goodin and B. M. Hoffman, *Biochemistry*, 1993, **32**, 4430.
5 J. E. Huyett, P. E. Doan, R. Gurbiel, A. L. P. Houseman, M. Sivaraja, D. B. Goodin and B. M. Hoffman, *J. Am. Chem. Soc.*, 1995, **117**, 9033.
6 M. Sivaraja, D. B. Goodin, M. Smith and B. M. Hoffman, *Science*, 1989, **245**, 738.
7 C. Essenmacher, S.-T. Kim, M.Atamian, G. T. Babcock and A. Sancar, *J. Am. Chem. Soc.*, 1993, **115**, 1602.
8 S.-T. Kim, A. Sancar, C. Essenmacher and G. T. Babcock, *Proc. Natl. Acad. Sci., USA*, 1993, **90**, 8023.
9 Y. F. Li, P. F. Heelis and A. Sancar, *Biochemistry*, 1991, **30**, 6322.
10 A. J. Baron, C. Stevens, C. Wilmot, K. D. Seneviratne, V. Blakeley, D. M. Dooley, S. E. V. Phillips, P. F. Knowles and M. J. McPherson, *J. Biol. Chem.*, 1994, **269**, 25095.
11 M. S. Ahmed, J. H. Parish and S. M. Hadi, *Carcinogenesis*, 1994, **15**, 1627.
12 J. Craggs, S. H. Kirk and S. 1. Ahmad, *J. Photochem. Photobiol. B: Biol.*, 1994, **24**, 123.

13 K. Hayashi, H. Amioka, J.-I. Kurokawa, Y. Kuga, S.-I. Nomura, Y. Ohkura, H. Ohtani and G. Kajiyama, *Scand. J. Gastroenterol.*, 1993, **28**, 261.
14 H. Z. Malina and X. D. Martin, *Graefe's Arch. Clin. Exper. Ophth.*, 1993, **231**, 483.
15 J. Murakami, M. Okazaki and T. Shiga, *Photochem. and Photobiol.*, 1989, **49**, 465.
16 G. J. Smith, *J. Photochem. Photobiol. B: Biol.*, 1994, **22**, 145.
17 D.-X. Tan, R. J. Reiter, L.-D. Chem, B. Poeggeler, L. C. Manchester and L. R. Barlow-Walden, *Carcinogenesis*, 1994, **15**, 215.
18 G. Dryhurst, *Chem. Rev.*, 1990, **90**, 791.
19 W. A. Creasey, in *Indoles Pt. Four: The Monoterpenoid Indole Alkaloids*, ed. J. E. Saxton, Wiley, New York, 1983, p. 783.
20 M. M. Salazar-Bookaman, I. Wainer and P. N. Patil, *J. Ocular Pharmacol.*, 1994, **10**, 217.
21 R. Foster and C. A. Fyfe, *J. Chem. Soc.* (*B*), 1966, 926.
22 R. Foster, *Organic Charge-Transfer Complexes*, Academic Press, London, 1969.
23 M. A. Slifkin, *Charge Transfer Interactions of Biomolecules*, Academic Press, London, 1971.
24 R. Holze and C. H. Hamann, *Tetrahedron*, 1991, **47**, 737.
25 K. Jackowska and J. Bukowska, *Pol. J. Chem.*, 1992, **66**, 1477.
26 K. M. Choi, J. H. Jang, H.-W. Rhee and K. H. Kim, *J. Appl. Poly. Sci.*, 1992, **46**, 1695.
27 K. M. Choi, C. Y. Kim and K. H. Kim, *J. Phys. Chem.*, 1992, **96**, 3782.
28 R. Arce, A. Grimison, J. Revuelta and G. A. Simpson, *Photochem. and Photobiol.*, 1975, **21**, 397.
29 A. I. Bokin, K. B. Petrushenko, V. K. Turchaninov, A. G. Gorshkov, A. S. Nakhmanovich and E. S. Domnina, *Zh. Obshch. Khim.* (*Engl. Trans.*), 1988, **58**, 905(803).
30 S. V. Jovanovic and S. Steenken, *J. Phys. Chem.*, 1992, **96**, 6674.
31 E. Leyva, M. S. Platz, B. Niu and J. Wirz, *J. Phys. Chem.*, 1987, **91**, 2293.
32 J. C. Mialocq, E. Amouyal, A. Bernas and D. Grand, *J. Phys. Chem.*, 1982, **86**, 3173.
33 G. Merényi, J. Lind and X. Shen, *J. Phys. Chem.*, 1988, **92**, 134.
34 X. Shen, J. Lind and G. Merényi, *J. Phys. Chem.*, 1987, **91**, 4403.
35 A. Harriman, *J. Phys. Chem.*, 1987, **91**, 6102.
36 K. B. Petrushenko, A. I. Vokin, V. K. Turchaninov and S. E. Korostova, *Izv. Akad. Nauk SSSR, Ser. Khim.* (*Engl. Trans.*), 1988, **58**, 41(32).
37 K. B. Petrushenko, A. I. Vokin and V. K. Terchaninov, *Isv. Akad. Nauk SSSR, Ser. Khim.* (*Engl. Trans.*), 1989, **59**, 31(23).
38 S. Solar, N. Getoff, P. S. Surdhar, D. A. Armstrong and A. Singh, *J. Phys. Chem.*, 1991, **95**, 3639.
39 E. F. McCord and S. G. Boxer, *Biochem. Biophys. R. Commun.*, 1981, **100**, 1436.
40 E. F. McCord, R. R. Bucks and S. G. Boxer, *Biochemistry*, 1981, **20**, 2880.
41 R. Consonni, A. D. Marco, G. Zannoni, L. Zetta and K. Dijkstra, *Gazz. Chim. Ital.*, 1989, **119**, 475.
42 S. Stob and R. Kaptein, *Photochem. and Photobiol.*, 1989, **49**, 565.
43 P. J. Hore and R. W. Broadhurst, *Prog. NMR Spectrosc.*, 1993, **25**, 345.
44 R. H. Bisby, S. A. Johnson, A. W. Parker and S. M. Tavender, *Time-resolved resonance Raman spectroscopy of indolyl and related radicals*, Ann. Rep., Central Laser Facility, Rutherford Appleton Laboratory, UK, 1995.
45 C. Berthomieu and A. Boussac, *Biospectrosc.*, 1995, **1**, 187.
46 S. E. Walden and R. A. Wheeler, *J. Phys. Chem.*, 1996, **100**, 1530; and in parts: *Abstr. Papers*, 50th Southwest Regional Meeting of the Am. Chem. Soc., Ft. Worth, TX, Am. Chem. Soc., Washington, DC, 1994, ORG 181; *Abstr. Papers*, 209th National Meeting of the Am. Chem. Soc., Anaheim, CA, Am. Chem. Soc., Washington, DC, 1995, PHYS 191; *Abstr. Papers*, 47th Southeast/51st Southwest Regional Meeting of the Am. Chem. Soc., Memphis, TN, Am. Chem. Soc., Washington, DC, 1995, ORG 504.
47 G. M. Jensen, D. B. Goodin and S. W. Bunte, *J. Phys. Chem.*, 1996, **100**, 954.
48 C. R. Johnson, M. Ludwig and S. A. Asher, *J. Am. Chem. Soc.*, 1986, **108**, 905.
49 J. C. Austin, T. Jordan and T. G. Spiro, in *Biomolecular Spectroscopy*, ed. R. J. H. Clark and R. E. Hester, Wiley, New York, 1993, pp. 55, and references therein.
50 S. E. Walden and R. A. Wheeler, preceding paper.
51 J. C. Slater, *Quantum Theory of Molecules and Solids*, McGraw-Hill, New York, 1974.
52 S. H. Vosko, L. Wilk and M. Nusair, *Can. J. Phys.*, 1980, **58**, 1200.
53 A. D. Becke, *Phys. Rev. A.*, 1988, **38**, 3098.
54 C. Lee, W. Yang and R. G. Parr, *Phys. Rev. B*, 1988, **37**, 785.
55 P. J. Stephens, F. J. Devlin, C. F. Chabalowski and M. J. Frisch, *J. Phys. Chem.*, 1994, **98**, 11623.
56 V. Barone, *Theor. Chim. Acta*, 1995, **91**, 113.
57 M. J. Cohen and D. P. Chong, *Chem. Phys. Lett.*, 1995, **234**, 405.
58 J. W. Finley and P. J. Stephens, *J. Mol. Struct., (THEOCHEM)*, 1995, **357**, 225.
59 Y. Qin and R. A. Wheeler, *J. Phys. Chem.*, 1996, **100**, 10554.
60 E. R. Davidson and D. Feller, *Chem. Rev.*, 1986, **86**, 681.
61 S. Boesch and R. A. Wheeler, *J. Phys. Chem.*, 1995, **99**, 8125.
62 N. Oliphant and R. J. Bartlett, *J. Chem. Phys.*, 1994, **100**, 6550.
63 R. S. Mulliken, *J. Chem. Phys.*, 1955, **23**, 1841.
64 R. S. Mulliken and W. C. Ermler, *Diatomic Molecules*, Academic, New York, 1977.
65 R. F. W. Bader, *Atoms in Molecules: A Quantum Theory*, Clarendon, Oxford, 1990.
66 X. Shen, J. Lind, T. E. Erikson and G. Merényi, *J. Chem. Soc., Perkin Trans. 2*, 1990, 597.
67 C. Adamo, V. Barone and A. Fortunelli, *J. Chem. Phys.*, 1995, **102**, 384.
68 Y. Qin and R. A. Wheeler, *J. Am. Chem. Soc.*, 1995, **117**, 6083.
69 Y. Qin and R. A. Wheeler, *J. Chem. Phys.*, 1995, **102**, 1689.
70 G. Rauhut and P. Pulay, *J. Phys. Chem.*, 1995, **99**, 3093.
71 G. Varsányi and S. Szöke, *Vibrational Spectra of Benzene Derivatives*, Academic, New York, 1969.
72 F. R. Dollish, W. G. Fateley and F. F. Bentley, *Characteristic Raman Frequencies of Organic Compounds*, Wiley, New York, 1974.
73 T. Kitagawa, *Prog. Biophys. Mol. Biol.*, 1992, **58**, 1.
74 H. Takeuchi and I. Harada, *Spectrochim. Acta, Part A*, 1986, **42**, 1069.
75 P. Pulay and F. Torok, *Acta Chim. Acad. Sci. Hung.*, 1966, **47**, 273.
76 G. Keresztury and G. Jalsovsky, *J. Molec. Struc.*, 1971, **10**, 304.
77 GAUSSIAN92/DFT, M. J. Frisch, G. M. Trucks, M. Head-Gordon, P. M. W. Gill, M. W. Wong, J. B. Foresman, B. G. Johnson, H. B. Schlegel, M. A. Robb, E. R. Replogle, R. Gomperts, J. L. Andres, K. Raghavachari, J. S. Binkley, C. Gonzalez, R. L. Martin, D. J. Fox, D. J. Defrees, J. Baker, J. J. P. Stewart and J. A. Pople, Gaussian, Inc., 1992.
78 GAUSSIAN94 (Revision B.3), M. J. Frisch, G. W. Trucks, H. B. Schlegel, P. M. W. Gill, B. G. Johnson, M. A. Robb, J. R. Cheeseman, R. A. Keith, G. A. Petersson, J. A. Montgomery, K. Raghavachari, M. A. Al-Laham, V. G. Zakrzewski, J. V. Ortiz, J. B. Foresman, J. Cioslowski, B. B. Stefanov, A. Nanayakkara, M. Challacombe, C. Y. Peng, P. Y. Ayala, W. Chen, M. W. Wong, J. L. Andres, E. S. Replogle, R. Gomperts, R. L. Martin, D. J. Fox, J. S. Binkley, D. J. Defrees, J. Baker, J. J. P. Stewart, M. Head-Gordon, C. Gonzalez and J. A. Pople, Gaussian, Inc., 1995.
79 M. W. Schmidt, K. K. Baldridge, J. A. Boatz, J. H. Jensen, S. Koseki, M. S. Gordon, K. A. Nguyen, T. L. Windus and S. T. Elbert, *QCPE Bull.*, 1990, **10**, 52.
80 M. Dupuis, D. Spangler and J. J. Wendoloski, *National Resource for Computations in Chemistry Software Catalog. Program QG01*, University of California, Berkeley, CA, 1980.
81 XMOL, Version 1.3.1, Research Equipment, Inc. d. b. a. Minnesota Supercomputer Center, Inc., 1993.
82 R. Barraza, M. Campos-Vallette, K. Figueroa, V. Manríquez and V. V. C., *Spectrochim. Acta, Part A*, 1990, **46**, 1375.
83 A. Lautié, M. F. Lautié, A. Gruger and S. A. Fakhri, *Spectrochim. Acta, Part A*, 1980, **36**, 85.
84 I. Harada, T. Miura and H. Takeuchi, *Spectrochim. Acta, Part A*, 1986, **42**, 307.
85 A. Y. Hirakawa, Y. Nishimura, T. Matsumoto, M. Nakanishi and M. Tsuboi, *J. Raman Spectrosc.*, 1978, **7**, 282.
86 W. J. Hehre, L. Radom, P. v. R. Schleyer and J. A. Pople, *Ab Initio Molecular Orbital Theory*, Wiley, New York, 1986.
87 I. N. Levine, *Quantum Chemistry*, Prentice-Hall, Englewood Cliffs, NJ, 1991.
88 W. Kohn and L. Sham, *Phys. Rev. A*, 1965, **140**, 1133.
89 P. Hohenberg and W. Kohn, *Phys. Rev. B*, 1964, **136**, 864.
90 M. J. S. Dewar and W. Thiel, *J. Am. Chem. Soc.*, 1977, **99**, 4899.
91 J. J. P. Stewart, *QCPE Bull.*, 1983, 455.
92 H. B. Schlegel, *J. Comput. Chem.*, 1982, **3**, 214.

Paper 6/03593K
Received 23*rd May* 1996
Accepted 6*th August* 1996